Clinical Investigation

Dual-Energy Computed Tomography-Enabled Material Separation

in Diagnosing Left Atrial Appendage Thrombus

Yu-Quan He, MD, PhD
Lin Liu, MD, PhD
Meng-Chao Zhang, MD, PhD
Hong Zeng, MD, PhD
Ping Yang, MD, PhD

We explored the potential clinical value of material separation enabled by dual-energy spectral computed tomography in detecting left atrial appendage thrombi.

The study enrolled 24 patients who were scheduled to undergo atrial fibrillation ablation (12 with and 12 without left atrial appendage thrombi). Computed tomograms were acquired in gemstone spectral imaging mode; the densities in the regions of the left atrial appendage cavities, pectinate muscles, and left atrial appendage thrombi were analyzed on monochromatic 70-keV images. Iodine and blood were chosen as the material basis pair; the iodine and blood densities were observed and quantitatively determined from the iodine- and blood-specific material decomposition images.

On the 70-keV monochromatic and iodine-specific images, the left atrial appendage pectinate muscles and thrombi appeared as areas of hypodense attenuation. On the blood-specific images, similar areas of high attenuation were observed in the thrombi and cavities, whereas lower attenuation was noticed in the pectinate muscles. The quantitative iodine and blood densities in the pectinate muscles were lower than those in the cavities (P <0.001). The iodine densities in the thrombi were lower than those in the cavities (P <0.001); however, blood densities did not differ significantly between the thrombi and cavities (P=0.192). Compared with the pectinate muscles, the thrombi showed lower blood-density differences (P=0.003) and higher iodine-density differences (P=0.006) in relation to the cavities.

Spectral computed tomography-enabled material separation is a novel method for differentiating left atrial appendage thrombi from pectinate muscles. The potential applications of this technology warrant further studies. ***(Tex Heart Inst J 2019;46(2):107-14)***

Key words: *Atrial appendage/diagnostic imaging; atrial fibrillation/complications; heart diseases/diagnostic imaging; image enhancement; image processing, computer-assisted/methods; predictive value of tests; radiography, dual-energy scanned projection/instrumentation; thrombosis/diagnostic imaging; tomography, x-ray computed/instrumentation/methods*

From: *Divisions of Cardiology (Drs. He, Yang, and Zeng) and Radiology (Drs. Liu and Zhang), China-Japan Union Hospital of Jilin University, Changchun, Jilin 130033, People's Republic of China*

Drs. He and Liu contributed equally to this study.

Address for reprints: *Hong Zeng, MD, PhD, Division of Cardiology, China-Japan Union Hospital of Jilin University, Cardiovascular Research Institute of Jilin Province, 126 Xiantai St., Changchun, Jilin 130033, PRC*

E-mail: *zenghong@jlu.edu.cn*

Left atrial appendage (LAA) thrombus formation is one of the most frequent complications that develop in patients with atrial fibrillation (AF). Because LAA thrombi are often accompanied by peripheral arterial thromboembolic events such as ischemic stroke, they are associated with high morbidity and mortality rates.[1] To date, transesophageal echocardiography (TEE) is the chief method for diagnosing LAA thrombi.[2] However, in addition to its relatively invasive nature, TEE yields results that depend greatly on the operator's skill and experience. Occasionally, LAA pectinate muscles and spontaneous echocardiographic contrast (SEC) are misidentified as LAA thrombi on TEE.[2] Cardiac computed tomography (CT) has been validated as an alternative method for identifying LAA thrombi; however, traditional multislice spiral CT is prone to false-positive findings when used to detect LAA thrombi.[3,4] A novel technology has recently been introduced in the form of dual-energy spectral CT, which uses a single X-ray tube and enables fast tube-voltage switching between low and high kilovoltage to simultaneously collect low- and high-energy data. In addition to yielding 101 monochromatic images, spectral CT can generate material-specific images based on the densities of material basis pairs, such as iodine and water, iodine and calcium, and calcium and fat, thereby enabling material separation and composition analysis.[5] Spectral CT technology has proved to be valuable in applications such as coronary artery imaging,[6] plaque detection,[7] and myocardial perfusion

This study was supported by research grants from the Health and Family Planning Commission of Jilin Province, China (No: 2014Z063), and the Science and Technology Bureau of Jilin Province, China (No. 20160101009JC).

imaging,[8] but it has rarely been used to diagnose cardiac thrombi.[9] In this study, we explored the applicability and potential clinical use of cardiac spectral CT imaging to differentiate LAA thrombi from LAA pectinate muscles. We based our analysis on the spectral differentiation of iodine and blood and the derived iodine- and blood-based material decomposition images. To our knowledge, this is the first reported use of spectral CT technology for this purpose.

Patients and Methods

A total of 24 patients who were scheduled to undergo radiofrequency ablation for AF at our hospital from April 2014 through October 2015 were consecutively enrolled in the study; the study population included 14 men and 10 women (mean age, 62.8 ± 9.6 yr; age range, 42–78 yr). All patients underwent TEE within 3 days before CT evaluation. The patients were divided into 2 groups on the basis of TEE results and were age- and sex-matched; each group included 7 men and 5 women (age range, 42–78 yr; mean age, 62.8 ± 9.8 yr). Group 1 consisted of 12 patients who did not have LAA thrombi or SEC. The duration of persistent AF in this group ranged from 6 months to 8 years; 2 patients had paroxysmal AF, 4 had persistent AF, and 6 had permanent AF. Group 2 consisted of 12 patients with LAA thrombi confirmed by TEE. The diagnosis of LAA thrombosis was further confirmed by serial TEE performed after systemic anticoagulation therapy was given. The duration of persistent AF in this group ranged from 8 months to 8 years; 2 patients had paroxysmal AF, 4 had persistent AF, and 6 had permanent AF. The LAA thrombi varied in size from a minimum of 6.2 × 4.5 mm to a maximum of 19.2 × 12.1 mm, as determined by TEE. All patients in Group 1 underwent radiofrequency ablation or balloon cryoablation for AF; no thromboembolic events occurred in this group intraoperatively or postoperatively. All patients in Group 2 received systemic anticoagulation with warfarin (Xinyi Pharmaceutical Co.), rivaroxaban (Bayer Schering Pharma AG), or dabigatran (Boehringer Ingelheim International GmbH). This study was conducted after we obtained informed consent from all human subjects and approval from the ethics committee of China-Japan Union Hospital of Jilin University.

Echocardiographic Evaluation

We used a Philips Sonos® 5500 ultrasound machine (Philips Electronics) with color-Doppler mode and a multiplane TEE probe, operated at a frequency of 5 MHz. After the LAA was clearly displayed, 0–180° continuous explorations were performed in various directions and at different depths. The LAA thrombus was defined as a solid, cloudy ultrasonic signal within the LAA cavity that was closely attached to the LAA wall, with margins that were distinguishable from the surrounding tissues and morphologies distinct from those of the LAA pectinate muscles and SEC (Fig. 1). We defined SEC as cloudy shadows with cyclotron motions within the LAA cavity, characterized by signals distinct from those of pseudonoises.

Spectral Computed Tomography

We used a Discovery CT750 HD multidetector spectral CT scanner (GE Healthcare) in gemstone spectral imaging (GSI) mode, with prospective electrocardiographic (ECG) gating. All patients signed an informed-consent form before undergoing CT imaging. The average heart rate of patients was 79 ± 14 beats/min. No β-adrenergic blocking agents were used to control the patients' heart rates, because the purpose of CT imaging was to evaluate the cardiac structures rather than the coronary arteries. While lying supine, each patient was connected to an ECG machine and a dual-head high-pressure injector. The scans were acquired from 1 to 2 cm below the tracheal carina extending to just below the diaphragm. A test bolus technique was used before image acquisition in each patient: a total of 20 mL of Omnipaque™ iodinated contrast agent (iohexol 350 mg/mL; GE Healthcare) was administered through the antecubital vein at a flow rate of 5 mL/s, and 15 mL of saline solution was subsequently administered at the same flow rate. A region of interest (ROI) was plotted into the aortic root, and a bolus time-density curve was acquired. The curve diagrams were analyzed immediately after the acquisitions, and the time to maximal enhancement scan delay was determined by adding 6 s to the time to maximal enhancement value. The patients were then instructed to hold their breath while 70 to 80 mL of iohexol was injected intravenously at the same flow rate, followed by 30 to 40 mL of saline solution. The CT image acquisition parameters were as follows: helical scan speed of X-ray tube, 0.6 s/cycle; pitch, 0.969; detector width, 40 mm; tube volt-

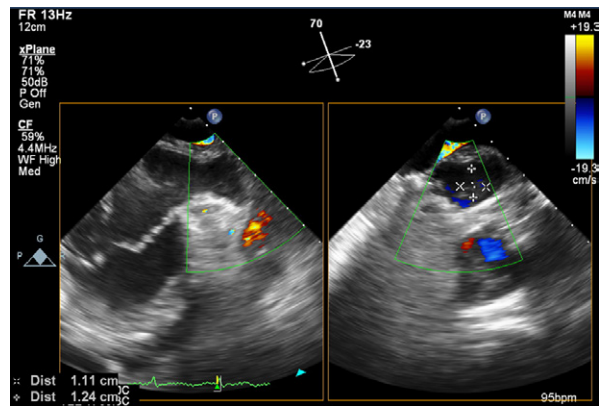

Fig. 1 *Transesophageal echocardiogram shows a 1.11 × 1.24-cm thrombus in the left atrial appendage cavity.*

age, instantaneous (0.5-ms) switch between high and low energy (140 and 80 kVp); tube current, 600 mA; rotation time, 0.35 s; layer thickness, 0.625 mm; and interlayer spacing, 0.625 mm. The scanning images were then reconstructed with use of the default 70-keV single-energy mode with a layer thickness and interlayer spacing of 0.625 mm. Image analysis and measurements were performed on an Advantage Workstation 4.6 (GE Healthcare).

Image Analysis and Measurements

Group 1

On the 70-keV monochromatic images, the image densities in the regions of the normal LAA cavities and the LAA pectinate muscles were simultaneously observed for each separate slice. The LAA pectinate muscles were identified as low-density shadows or filling defects within the iodine-enhanced LAA cavities (Fig. 2A). Iodine and blood were selected as the material basis pair in the GSI viewer software. We simultaneously observed the iodine and blood densities in the regions of the LAA cavities and pectinate muscles on the iodine- and blood-specific material decomposition images. Subsequently, a scanning slice showing clear images and the maximum pectinate muscle area was selected on the axial 70-keV monochromatic images, and 1 × 1-mm ROIs were selected for the regions of the LAA pectinate muscles and the LAA cavities. The same ROIs were automatically copied to the exact same locations on the iodine- and blood-specific images, and the iodine and blood densities at these ROIs were quantitatively measured. Three ROIs were selected for each slice in the normal LAA cavities and pectinate muscles, respectively, and the quantitative measurements were repeated for 10 scanning slices. The averaged results of the iodine and blood densities were used in the final statistical analysis.

To further illustrate the differences between the iodine and blood densities of the LAA pectinate muscles and the LAA cavities, we inserted additional 1 × 1-mm ROIs in the central regions of the LAA pectinate muscles and the LAA cavities, and we calculated the differences in blood and iodine density by subtracting the blood and iodine densities in the central regions of the LAA pectinate muscles from those of their respective LAA cavities for each slice. This process was repeated for 10 scanning slices, and the averaged results were used as the patients' final differences in iodine and blood densities between the LAA pectinate muscles and LAA cavities.

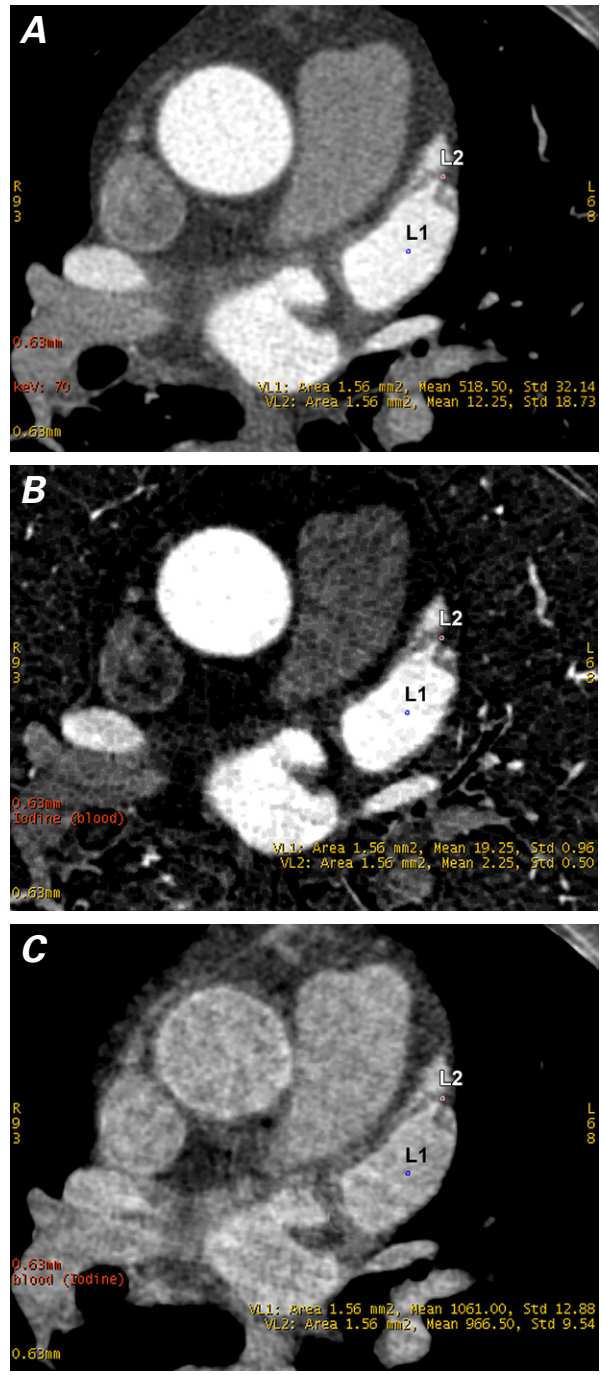

Fig. 2 *In a patient without left atrial appendage (LAA) thrombus, spectral computed tomography was used to produce* ***A****) a reconstructed 70-keV monochromatic image;* ***B****) a decomposed iodine-specific image, and* ***C****) a decomposed blood-specific image. L1 and L2 are the regions of interest in the LAA cavity and the pectinate muscles, respectively. The LAA pectinate muscles show lower attenuation than does the LAA cavity.*

Group 2

Using the same method as for Group 1, we simultaneously observed the image densities in the regions of the LAA thrombi and the LAA cavities on the axial 70-keV monochromatic images for each slice. We identified LAA thrombi as uneven low-attenuation areas or filling defects within the LAA cavity, with morphologies distinct from those of the LAA pectinate muscles and CT artifacts. Two attending radiologists (LL and MCZ) and one TEE expert (DMG or JS) identified the LAA

thrombi together. Using the iodine- and blood-specific material decomposition images, we performed simultaneous comparative observation of the iodine and blood densities in the regions of the LAA thrombi and the LAA cavities and quantitatively measured the averaged iodine and blood concentrations in the LAA thrombi and cavities. Similarly, the iodine- and blood-density differences between the LAA thrombi and the LAA cavities were obtained by subtracting the blood and iodine densities in the central regions of the LAA thrombi from those of their respective LAA cavities for each slice.

We planned simultaneous determination of the iodine and blood densities of the LAA thrombi and the pectinate muscles in this group of patients. However, because we were unable to identify the pectinate muscles on the slices displaying the LAA thrombi, we determined only the iodine- and blood-specific densities of the LAA thrombotic lesions and cavities for each slice, without measuring those of the pectinate muscles.

Statistical Analysis

SigmaStat® 3.5 software (Systat Software, Inc.) was used for statistical analyses. Quantitative data are expressed as mean ± SD for continuous variables with normal distribution. Data are expressed as median (25th–75th percentile) for continuous variables without normal distribution. The paired Student *t* test was used to compare the blood and iodine densities between the LAA cavities and thrombi and between the LAA cavities and pectinate muscles for each slice. An independent-sample *t* test was used to compare the iodine and blood densities and the iodine- and blood-density differences between groups. The nonparametric Mann-Whitney test was used to compare samples without a normal distribution. *P* values <0.05 were considered statistically significant.

Results

Group 1

On visual evaluation, the LAA cavities with normal filling of iodinated contrast medium showed high attenuation on the 70-keV monochromatic (Fig. 2A) and the iodine-specific images (Fig. 2B), whereas the LAA pectinate muscles appeared as areas of hypodense attenuation or filling defects. On the blood-specific images, the LAA pectinate muscles showed lower attenuation than did the LAA cavities on visual evaluation (Fig. 2C). The quantitative iodine and blood concentrations in the regions of the LAA pectinate muscles were significantly lower than those of the LAA cavities: iodine density, 5.74 ± 2.4 vs 16.64 ± 3.06 mg/cm^3 (*P* <0.001); and blood density, 1,002.37 ± 20.6 vs 1,047.53 ± 11.88 mg/cm^3 (*P* <0.001) (Table I).

Group 2

On visual evaluation, the LAA cavities with normal filling of iodinated contrast medium showed high attenuation on the 70-keV monochromatic (Fig. 3A) and the iodine-specific images (Fig. 3B), whereas LAA thrombi appeared as areas of low attenuation or filling defects. On the blood-specific images, comparable areas of high attenuation were observed in the LAA cavities and thrombi (Fig. 3C). The quantitative iodine concentrations were lower in the regions of the LAA thrombi than in the LAA cavities (1.77 ± 1.53 vs 16.96 ± 4.83 mg/cm^3; *P* <0.001), whereas the quantitative blood concen-

TABLE I. Comparison of Iodine and Blood Densities and Differences in Densities between the Regions of the LAA Thrombi and Pectinate Muscles and their Respective LAA Cavities in Patients with and without LAA Thrombi

	Group 1 (n=12)			**Group 2** (n=12)			
Variable	**LAA Cavities** (mg/cm^3)	**Pectinate Muscles** (mg/cm^3)	***P* Value**	**LAA Cavities** (mg/cm^3)	**LAA Thrombi** (mg/cm^3)	***P* Value**	***P* Value***
Blood density	1,047.53 ± 11.88	1,002.37 ± 20.6	<0.001	1,046.74 ± 10.68	1,036.25 ± 24.87	0.192	0.001
Iodine density	16.64 ± 3.06	5.74 ± 2.4	<0.001	16.96 ± 4.83	1.77 ± 1.53	<0.001	<0.001
Blood-density differences	—	41.28 (34.5–47.69)	—	—	9.55 (–0.08 to 23.84)	—	0.003
Iodine-density differences	—	10.74 ± 2.14	—	—	15.19 ± 4.65	—	0.006

LAA = left atrial appendage

*LAA thrombi vs pectinate muscles

The blood-density differences were calculated by subtracting the blood densities in the central regions of the LAA pectinate muscles and thrombi from those of their respective LAA cavities for every slice. The iodine-density differences were calculated by subtracting the iodine densities in the central regions of the LAA pectinate muscles and thrombi from those of their respective LAA cavities for every slice.

Data are presented as mean ± SD or as median (25th–75th percentile). *P* <0.05 was considered statistically significant.

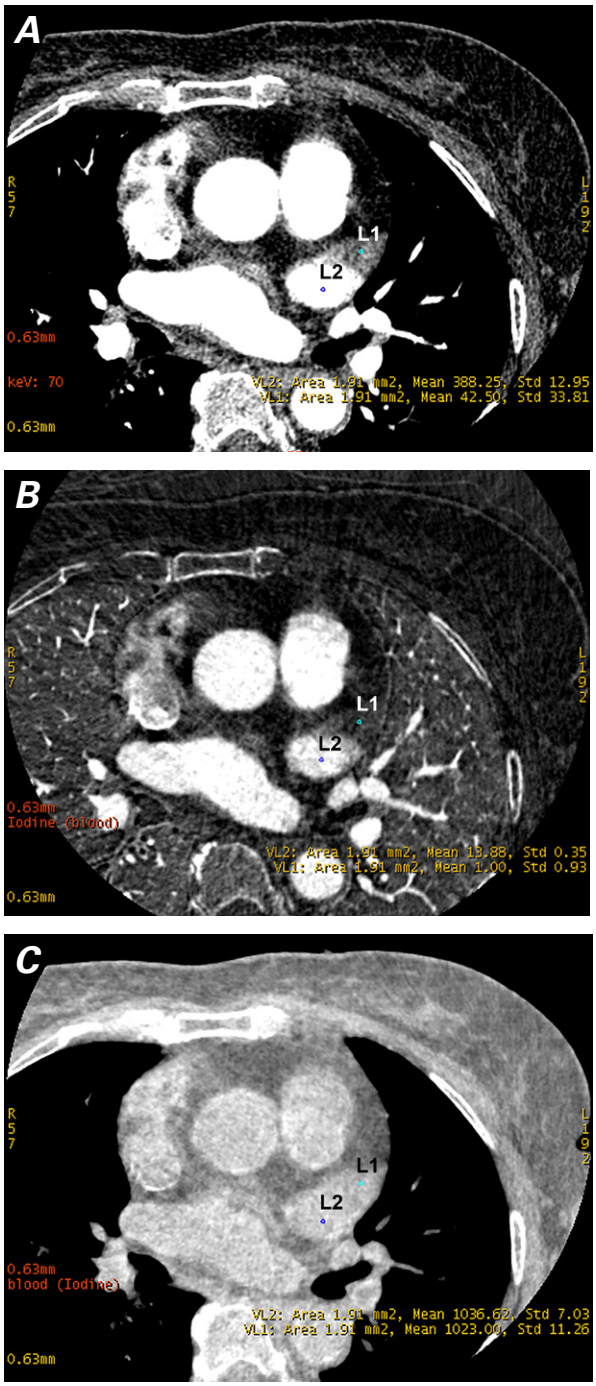

Fig. 3 *In a patient with left atrial appendage (LAA) thrombus, spectral computed tomography was used to produce* ***A****) a reconstructed 70-keV monochromatic image;* ***B****) a decomposed iodine-specific image; and* ***C****) a decomposed blood-specific image. L1 and L2 are the regions of interest in the LAA thrombus and the LAA cavity, respectively. In comparison with the LAA cavity, the LAA thrombus shows lower attenuation in A and B; conversely, areas of higher attenuation are observed in C.*

trations did not differ significantly between the LAA thrombi and the cavities (1,036.25 ± 24.87 vs 1,046.74 ± 10.68 mg/cm^3; *P*=0.192) (Table I).

The LAA thrombi in Group 2 showed a higher blood density (1,036.25 ± 24.87 vs 1,002.37 ± 20.6 mg/cm^3; *P*=0.001) and a lower iodine density (1.77 ± 1.53 vs 5.74 ± 2.4 mg/cm^3; *P* <0.001) than did the LAA pectinate muscles in Group 1. In addition, the statistical analysis showed that the LAA thrombi in Group 2 had lower blood-density differences and higher iodine-density differences in relation to the LAA cavities than with the LAA pectinate muscles in Group 1: blood-density differences, 9.55 (–0.08 to 23.84) vs 41.28 (34.5–47.69) mg/cm^3 (*P*=0.003); and iodine-density difference, 15.19 ± 4.65 vs 10.74 ± 2.14 mg/cm^3 (*P*=0.006) (Table I).

Discussion

Left atrial appendage thrombosis is a frequent complication in patients with AF.[1] An LAA thrombus is defined as a solid lumpy mass that is closely attached to the LAA wall, with well-defined margins that are distinguishable from the surrounding tissues and a morphology that can be differentiated from that of the LAA pectinate muscles and from technological artifacts.[10] The thrombosis is associated with high morbidity and mortality rates because it often occurs simultaneously with peripheral arterial thromboembolic events such as ischemic stroke.[1] The thrombus can be substantially reduced in size or even completely dissolved if effective anticoagulation is administered in a timely fashion.[1] In addition, LAA thrombosis is an absolute contraindication for interventions such as AF ablation and LAA closure.[11] Therefore, accurate and timely detection of an LAA thrombus is crucial to optimal treatment and improving patients' prognoses.

Transesophageal echocardiography has been validated as a fairly accurate method for identifying LAA thrombi and is currently the gold standard for the diagnosis of these lesions. Manning and colleagues[12] conducted an intraoperative study and found that TEE had a sensitivity of 100%, a specificity of 99%, a positive predictive value of 86%, and a negative predictive value of 100% for the diagnosis of LAA thrombi.[12] However, TEE is a semi-invasive technique associated with rare but potentially life-threatening complications.[13] In addition, TEE results depend greatly on the operator's skill and experience. Furthermore, normal LAA pectinate muscles or SEC are sometimes misdiagnosed as LAA thrombi on TEE.[2] Cardiac magnetic resonance imaging has been proposed as an alternative method for the diagnosis of LAA thrombi; however, it has several limitations, including lower imaging speed, higher cost, longer examination time, and some contraindications.[14] Multislice spiral CT is a widely used noninvasive diagnostic method with multiple advantages. In addition to its high scanning speed and high resolution, it enables simultaneous 3-dimensional imaging of the coronary arteries, left atrium, pulmonary veins, esophagus, and

phrenic nerves.[15,16] However, because the normal LAA pectinate muscles appear as low-density shadows that are like LAA thrombi on traditional CT images, differentiating between these structures and LAA thrombotic lesions has been challenging for clinicians.[3,4,17]

A meta-analysis conducted by Romero and colleagues[18] showed that multislice CT delayed scanning is a reliable alternative to TEE for diagnosing LAA thrombi, with sensitivity, specificity, and positive and negative predictive values >92%.[16] Hur and associates[19,20] further improved the delayed-scanning techniques for differentiating between LAA thrombi and SEC. Hur and colleagues[21] used dual-energy CT scanning and found that the quantitative iodine (water) density was significantly lower in LAA thrombus than in SEC. Receiver operating characteristic (ROC) analysis indicated that a cutoff of 1.74 mg/mL provided a sensitivity and a specificity of 100% for differentiating LAA thrombi from SEC, with an area under the curve of 1.[21]

The abovementioned CT imaging algorithm improved the ability to distinguish between LAA thrombi and SEC; however, it might not be helpful in differentiating LAA thrombotic lesions from normal LAA pectinate muscles. The current standard method for the diagnosis of LAA thrombi, TEE, also has limitations and can yield false-positive results.[22] The anatomic complexity of the LAA, which includes multiple branches, uneven walls, and pectinate muscles,[23] leaves normal LAA structures susceptible to misidentification as LAA thrombi when TEE or CT is used.[17-20,22] Hypertrophy of the LAA pectinate muscle often occurs in patients who have AF because of myocardial remodeling, and when an irregular and pectinate muscle-like LAA thrombus coexists with enlarged pectinate muscles in the same LAA cavity, differentiating between these structures becomes even more difficult.[23] In addition, the normal membranous or ridgelike structures near the orifices of the left superior pulmonary vein and the LAA have been easily misdiagnosed as thrombi on TEE.[24]

Spectral CT is a novel diagnostic technology and a qualitative leap forward in the field of radiology.[5-8] Unlike conventional CT, which is limited to CT number measurement, this technology enables a multiparameter imaging approach, offering an alternative to magnetic resonance imaging. In this study, we used a high-definition CT scanner in GSI mode, with a single X-ray tube and instantaneous fast switching between low and high voltages (80 and 140 kVp) to obtain the reconstructed 70-keV monochromatic images. We found that obtaining separate iodine- and blood-specific material decomposition images facilitated the differentiation between LAA thrombotic lesions and pectinate muscles. To our knowledge, this is the first reported use of spectral CT technology for this purpose.

In this study, we noticed that both LAA thrombi and pectinate muscles appeared as low-density shadows on the 70-keV monochromatic images. Similarly, on the iodine-specific images, LAA thrombi and pectinate muscles were both visually observed as areas of low attenuation or filling defects. The quantification of iodine concentrations, which were lower in the regions of the LAA thrombi and pectinate muscles than in the LAA cavities, confirmed these visual findings. On the blood-specific images, there were differences between the appearance of the LAA thrombi and that of the pectinate muscles; comparable areas of high attenuation were observed in the LAA thrombi and the LAA cavities, whereas lower attenuation was noted in the LAA pectinate muscles. The quantified blood concentrations in the LAA thrombi were like those in the LAA cavities, whereas lower blood concentrations were noted in the LAA pectinate muscles than in the LAA cavities. By simultaneously comparing the blood- and iodine-specific images slice by slice, we could easily differentiate an LAA thrombus from normal LAA pectinate muscles. This is impossible to achieve when using traditional multislice spiral CT technology.

The differences between the LAA thrombi and pectinate muscles on the blood- and iodine-specific material decomposition images may be explained by differences in the composition of the materials and in blood-supply characteristics. Iodine is the key component of the contrast material most often used in contrast-enhanced CT. Dual-energy CT enables the evaluation of iodine distribution by creating iodine-specific images. The iodinated contrast agent may not easily reach the areas of the LAA pectinate muscles and thrombi, which are characterized by reduced or sluggish blood flow. Therefore, in comparison with the LAA cavity, which fills with the iodinated contrast agent rapidly, the LAA pectinate muscles and thrombi exhibit slight or no enhancement on the iodine-specific images. It may be even more difficult for the iodinated contrast agent to reach the central areas of LAA thrombi than to reach pectinate muscles; therefore, LAA thrombi may have lower iodine concentrations and higher iodine-density differences in relation to the LAA cavity than do the LAA pectinate muscles, as shown in this study.

The LAA thrombus is a solid mass that contains aggregated blood components from within the LAA cavity, so its composition is quite like the blood circulating in the cavity (for example, both contain erythrocytes and platelets). Therefore, the observed attenuation and measured blood concentrations of the LAA thrombi are like those of the LAA cavities on the blood-specific material decomposition images. On the other hand, LAA pectinate muscles mainly comprise fibrous tissue and smooth muscle, which differ substantially from the clot and blood components in the LAA cavity. Thus, the observed attenuation and measured blood concentrations in the LAA pectinate muscles are quite different from those of the LAA thrombi and cavities on the

blood-specific images. It is this principle that enables the differentiation between LAA thrombi and pectinate muscles on the basis of simple visual evaluation and quantitative density measurement.

Currently, both TEE and CT evaluations are necessary before AF ablation. The TEE evaluation reveals the cardiac thrombi, and multislice CT anatomic reconstructions of the left atrium and pulmonary veins guide the isolation procedure. Widely used 3-dimensional electroanatomic mapping systems such as the CARTO®3 system (Biosense Webster, a Johnson & Johnson company) or the EnSite Precision™ cardiac mapping system (Abbott) integrate the reconstructed CT images with those of the electrophysiologic maps, reinforcing the use of CT for routine evaluation before AF ablation. We anticipate that a spectral CT "one-stop" imaging technique may provide detailed anatomy of the coronary arteries, left atrium, pulmonary veins, esophagus, and phrenic nerves while meeting the clinical requirements for the diagnosis of LAA thrombi. This technology could benefit patients by replacing semi-invasive TEE before AF ablation and may, therefore, have clinical value in this context.

Dual-energy CT-enabled material separation technology with its generation of blood- and iodine-specific images provides a novel, simple, and feasible method to differentiate between LAA thrombi and pectinate muscles. The potential applications of this technology in clinical practice warrant further research.

Study Limitations

The main limitation of this study was the small size of our sample, so our findings should be interpreted as a proof of principle, which shows the feasibility of using dual-energy spectral CT-enabled material separation to distinguish LAA thrombi from pectinate muscles. Larger studies in which investigators are blinded to TEE results are necessary to validate the current results and to establish the cutoff and reference values for normal and abnormal blood-density differences between the LAA thrombus and pectinate muscles and the LAA cavity.

Ideally, we should have simultaneously determined the iodine and blood densities of the LAA thrombi and pectinate muscles in the patients in Group 2. However, because we were unable to detect pectinate muscles and LAA thrombotic lesions in the same slice, we compared only the iodine- and blood-specific densities of the LAA thrombi to those of their respective cavities for each slice and did not measure those of the pectinate muscles. We also found relatively large between-subject variability in the blood and iodine densities, which may be attributed to differences in thrombus formation time and embolus composition among individuals; however, we observed significant differences in the quantified blood and iodine densities for LAA thrombi and pectinate muscles—and, of note, these differences were obvious from mere visual evaluation. In addition, TEE examination was considered the gold standard for diagnosing LAA thrombi in this study, and diagnoses were not confirmed by surgery and histopathology. Another challenge of using the CT imaging technique that we describe is differentiating between LAA thrombi and stasis; however, patients with both AF and SEC were not enrolled in this study. Finally, we found that the blood-iodine material basis pair is a valuable marker of LAA thrombus. However, the selection and combination of material pairs are crucial in the differential diagnosis of tissue components, so additional substance pairs should be explored in future studies.

Acknowledgments

The authors thank 2 experts at the Ultrasonography Department of our hospital—Dong-Mei Gao, MD, PhD, and Jun Song, MD, PhD—for their role in the identification of pectinate muscles and LAA thrombotic lesions on TEE.

References

1. Fukuda S, Watanabe H, Shimada K, Aikawa M, Kono Y, Jissho S, et al. Left atrial thrombus and prognosis after anticoagulation therapy in patients with atrial fibrillation. J Cardiol 2011;58(3):266-77.
2. Anter E, Silverstein J, Tschabrunn CM, Shvilkin A, Haffajee CI, Zimetbaum PJ, et al. Comparison of intracardiac echocardiography and transesophageal echocardiography for imaging of the right and left atrial appendages. Heart Rhythm 2014;11(11):1890-7.
3. Shapiro MD, Neilan TG, Jassal DS, Samy B, Nasir K, Hoffmann U, et al. Multidetector computed tomography for the detection of left atrial appendage thrombus: a comparative study with transesophageal echocardiography. J Comput Assist Tomogr 2007;31(6):905-9.
4. Zou H, Zhang Y, Tong J, Liu Z. Multidetector computed tomography for detecting left atrial/left atrial appendage thrombus: a meta-analysis. Intern Med J 2015;45(10):1044-53.
5. Danad I, Fayad ZA, Willemink MJ, Min JK. New applications of cardiac computed tomography: dual-energy, spectral, and molecular CT imaging. JACC Cardiovasc Imaging 2015;8(6):710-23.
6. Fuchs TA, Stehli J, Fiechter M, Dougoud S, Gebhard C, Ghadri JR, et al. First experience with monochromatic coronary computed tomography angiography from a 64-slice CT scanner with gemstone spectral imaging (GSI). J Cardiovasc Comput Tomogr 2013;7(1):25-31.
7. Zainon R, Ronaldson JP, Janmale T, Scott NJ, Buckenham TM, Butler AP, et al. Spectral CT of carotid atherosclerotic plaque: comparison with histology. Eur Radiol 2012;22(12):2581-8.
8. Fahmi R, Eck BL, Levi J, Fares A, Dhanantwari A, Vembar M, et al. Quantitative myocardial perfusion imaging in a porcine ischemia model using a prototype spectral detector CT system. Phys Med Biol 2016;61(6):2407-31.
9. Zeng H, Zhang MC, He YQ, Liu L, Tong YL, Yang P. Application of spectral computed tomography dual-substance sepa-

ration technology for diagnosing left ventricular thrombus. J Int Med Res 2016;44(1):54-66.
10. Patti G, Pengo V, Marcucci R, Cirillo P, Renda G, Santilli F, et al. The left atrial appendage: from embryology to prevention of thromboembolism. Eur Heart J 2017;38(12):877-87.
11. Naksuk N, Padmanabhan D, Yogeswaran V, Asirvatham SJ. Left atrial appendage: embryology, anatomy, physiology, arrhythmia and therapeutic intervention. JACC Clin Electrophysiol 2016;2(4):403-12.
12. Manning WJ, Weintraub RM, Waksmonski CA, Haering JM, Rooney PS, Maslow AD, et al. Accuracy of transesophageal echocardiography for identifying left atrial thrombi. A prospective, intraoperative study. Ann Intern Med 1995;123 (11):817-22.
13. Chan KL, Cohen GI, Sochowski RA, Baird MG. Complications of transesophageal echocardiography in ambulatory adult patients: analysis of 1500 consecutive examinations. J Am Soc Echocardiogr 1991;4(6):577-82.
14. Rathi VK, Reddy ST, Anreddy S, Belden W, Yamrozik JA, Williams RB, et al. Contrast-enhanced CMR is equally effective as TEE in the evaluation of left atrial appendage thrombus in patients with atrial fibrillation undergoing pulmonary vein isolation procedure. Heart Rhythm 2013;10(7):1021-7.
15. Tops LF, Krishnan SC, Schuijf JD, Schalij MJ, Bax JJ. Noncoronary applications of cardiac multidetector row computed tomography. JACC Cardiovasc Imaging 2008;1(1):94-106.
16. Wang YJ, Liu L, Zhang MC, Sun H, Zeng H, Yang P. Imaging of pericardiophrenic bundles using multislice spiral computed tomography for phrenic nerve anatomy. J Cardiovasc Electrophysiol 2016;27(8):961-71.
17. Nakanishi T, Hamada S, Takamiya M, Naito H, Imakita S, Yamada N, et al. A pitfall in ultrafast CT scanning for the detection of left atrial thrombi. J Comput Assist Tomogr 1993; 17(1):42-5.
18. Romero J, Husain SA, Kelesidis I, Sanz J, Medina HM, Garcia MJ. Detection of left atrial appendage thrombus by cardiac computed tomography in patients with atrial fibrillation: a meta-analysis. Circ Cardiovasc Imaging 2013;6(2):185-94.
19. Hur J, Kim YJ, Lee HJ, Nam JE, Ha JW, Heo JH, et al. Dual-enhanced cardiac CT for detection of left atrial appendage thrombus in patients with stroke: a prospective comparison study with transesophageal echocardiography. Stroke 2011;42(9):2471-7.
20. Hur J, Kim YJ, Lee HJ, Ha JW, Heo JH, Choi EY, et al. Left atrial appendage thrombi in stroke patients: detection with two-phase cardiac CT angiography versus transesophageal echocardiography. Radiology 2009;251(3):683-90.
21. Hur J, Kim YJ, Lee HJ, Nam JE, Hong YJ, Kim HY, et al. Cardioembolic stroke: dual-energy cardiac CT for differentiation of left atrial appendage thrombus and circulatory stasis. Radiology 2012;263(3):688-95.
22. Khandheria BK, Seward JB, Tajik AJ. Critical appraisal of transesophageal echocardiography: limitations and pitfalls. Crit Care Clin 1996;12(2):235-51.
23. Yamamoto M, Seo Y, Kawamatsu N, Sato K, Sugano A, Machino-Ohtsuka T, et al. Complex left atrial appendage morphology and left atrial appendage thrombus formation in patients with atrial fibrillation. Circ Cardiovasc Imaging 2014;7(2):337-43.
24. Blanchard DG, Dittrich HC, Mitchell M, McCann HA. Diagnostic pitfalls in transesophageal echocardiography. J Am Soc Echocardiogr 1992;5(5):525-40.